Green Chemistry

PAPER

View Article Online
View Journal | View Issue

Cite this: *Green Chem.*, 2024, **26**, 1577

Screening of ionic liquids for the dissolution of chitosan using COSMO-RS†

Shue Yee Mok, [a] Magaret Sivapragasam,*[b] Maisara Shahrom Raja Shahrom,[b] Mohammad Azmi Bustam @ Khalil[c] and Zurina Zainal Abidin[d]

Received 22nd September 2023,
Accepted 8th December 2023

DOI: 10.1039/d3gc03586g

rsc.li/greenchem

The dissolution of chitosan is a tedious and time-consuming process. Herein, we select the best Ionic Liquids (ILs) for chitosan dissolution through the application of Conductor-like Screening Model for Real Solvents (COSMO-RS), which allowed the screening of 640 ILs based on 32 cations based on amino acids, imidazolium, pyridinium, and pyrrolidinium, and 20 selected anions such as [$C_2H_3O_2$], [Cl], [NO_3], [BF_4], and others. Thermodynamic properties such as logarithmic activity coefficient at infinite dilution ($\ln\gamma$) and excess enthalpy (H^E) were used to evaluate the dissolution potential of ILs towards chitosan, whereby low values of $\ln\gamma$ and H^E indicated better engagement between the solute and the solvent, thus resulting in a higher solute being dissolved. A preliminary screening of chitosan dissolution was carried out in all 5 synthesized ILs to validate the results obtained by COSMO-RS. It was observed that ILs with [BF_4^-] as the anion and cations such as [Ser], [Gly], [Phe], [Cys], and [Asn] have the lowest $\ln\gamma$ values, hence better interaction with chitosan. The values of H^E indicated that the molecular interactions between chitosan and ILs were governed by hydrogen bonding (ranging from 37 to 50%), followed by misfit interactions (ranging from 21 to 31%) and van der Waals forces (ranging from 22 to 32%) due to the abundance of hydroxyl (–OH) groups present in the intermolecular and intramolecular chitosan structures. These proved the great ability of COSMO-RS to accurately predict the dissolution of chitosan in ILs.

1. Introduction

Chitosan is a linear polysaccharide of marine origin that is mainly composed of *N*-acetyl-D-glucosamine and D-glucosamine monomers connected by a β-1,4-glycosidic bond.[1] Naturally, it can be extracted from fungal cell walls, but most of the chitosan available in the industry is produced by partial deacetylation of chitin using concentrated alkali.[2] Chitosan has been widely used in multi-industry applications such as medical,[3,4] pharmaceutical,[5,6] agricultural,[7,8] cosmetics,[9,10] and other industries, owing to its special characteristics of biocompatibility, biodegradability into harmless products, non-toxicity, shape flexibility, and antimicrobial properties.[11] However, the usage of chitosan constitutes a major limitation owing to its insolubility in water and most organic solvents due to the extensive intermolecular and intramolecular hydrogen bonds present within its chemical structure.[12] Chitosan solution is usually made using dilute aqueous acidic solutions due to its ability to act as a weak base and the protonation of amino groups on C(2) of D-glucosamine monomers.[13] Nevertheless, acids are highly volatile and toxic in nature, providing a non-sustainable approach to the dissolution of chitosan. Thus, a more feasible method to solubilize chitosan is very much needed. Over the past two decades, Ionic Liquids (ILs) have been proposed as alternative solvents to dissolve chitosan, which has been observed in the work of Xie *et al.*,[14] Zhang *et al.*,[15] Chen *et al.*,[16] and Sun *et al.*,[17] using a series of imidazolium-based ILs.

Ionic Liquids (ILs) are a group of salts composed of organic cations and organic/inorganic anions with a melting point below 100 °C and distinctive characteristics of negligible vapour pressure, thermal and chemical stability, high solvation potential, and recyclability.[18–20] The most remarkable feature of ILs is their innumerable cation–anion combinations. Ionic Liquids (ILs) have been used mostly in industrial applications such as electrochemistry,[21] gas capture,[22] catalysis,[23] separation,[24] and dissolution,[17] as well as in medicinal and pharmaceutical sectors such as DNA preservation,[25] diagnostic

[a]*School of Postgraduate Studies, Research and Internalisation (SPRINT), Faculty of Integrated Life Sciences, Quest International University, 30250 Ipoh, Perak, Malaysia*
[b]*School of Integrated Sciences, Faculty of Integrated Life Sciences, Quest International University, 30250 Ipoh, Perak, Malaysia. E-mail: magaret_62@yahoo.co.uk*
[c]*Centre of Research in Ionic Liquids, Universiti Teknologi PETRONAS, 32610 Seri Iskandar, Perak, Malaysia*
[d]*Department of Chemical and Environmental Engineering, Faculty of Engineering, Universiti Putra Malaysia, 43400 Serdang, Selangor, Malaysia*
† Electronic supplementary information (ESI) available. See DOI: https://doi.org/10.1039/d3gc03586g

tools,[26] and drug delivery systems.[27] The wide range of applications of ILs is made possible by the extensive choice of cations and anions and the ability to design an IL specific for a particular task. However, it has become a challenging task to determine the right combination of cations and anions, particularly in the dissolution of chitosan. Hence, a computational tool for the screening of potential ILs is essential to enhance the process's efficiency.

An initial pre-screening of ILs is indispensable when it comes to dissolving chitosan. This is because there are still numerous ILs with a great solvation capability waiting to be uncovered. In this context, a simulation tool known as Conductor-like Screening Model for Real Solvents (COSMO-RS) has gained significant traction in various research fields such as gas capture and separation,[28,29] denitrification,[30] extraction,[31] and dissolution[32,33] due to its ability to accurately predict the thermodynamic properties of ILs without relying on the actual experimental data. Notably, COSMO-RS has been employed in the evaluation of ILs to dissolve solutes such as cellulose,[32] hemicellulose,[34] keratin,[33] artemisinin,[35] and plastics,[36] yielding accurate and reliable results.

In this study, COSMO-RS has been employed to design and screen suitable ILs for the dissolution of chitosan. It is worth highlighting that, up to this point, the COSMO-RS model has not been utilized to study the interaction between chitosan and ILs. To accomplish this, we have screened a total of 32 cations comprising amino acids, imidazolium, pyridinium, and pyrrolidinium with 20 anions based on previous studies[14,17,32–35,37,38] for the solubilization of chitosan. Amino acid cations were selected as they can dissolve a wider range of chitosan at different molecular weights at ambient temperature with a lower viscosity,[37] while cations such as imidazolium, pyridinium, and pyrrolidinium were selected as reference cations because they have been typically used to dissolve chitosan.[14,17,38] A wide range of anions such as carboxylates, aromatic carboxylates, halogens, organic acids, sulphur-containing anions and nitrogen-containing anions were coupled with the cations in the screening of ILs for chitosan dissolution and these anions were also commonly used in IL screening in the dissolution of cellulose,[32] keratin,[33] artemisinin,[34] and plastics.[35] Appropriate cation–anion coordination was selected based on the values of the logarithmic activity coefficient at infinite dilution and excess enthalpy, which provides an insight into the ILs' ability to dissolve chitosan effectively. The ILs recommended by the COSMO-RS software were synthesized and experimentally validated to prove the efficacy of COSMO-RS in accurately predicting chitosan dissolution behaviour.

2. Experimental

2.1 Geometry optimization of chitosan, cations and anions

The molecular geometries of chitosan, amino acid cations, and anions were optimized using the software, Tmole*X* ver. 4.4.1 (COSMOlogic GmbH & Co. KG, Leverkusen, Germany) through quantum and energy calculations. Prior to the geometry optimization, the simplified molecular input line entry system (SMILES) codes of the chitosan, cations, and anions were obtained from the PubChem database (NCBI, USA) and input in the software as a three-dimensional structure. Quantum calculations were performed using the density functional theory (DFT) level, while energy calculations were conducted using Becke, 3-parameter, the Lee–Yang–Parr (B3LYP) functional with resolution of identity (RI) approximation and the triple-ζ valence polarization basis set.

2.2 COSMO-RS analysis

All the COSMO files generated through geometry optimization were used as the input files for COSMO-RS calculations through COSMO*therm*X ver. 19.0.1 (COSMOlogic GmbH & Co. KG, Leverkusen, Germany) software, utilizing the parametrization BP_TZVP_19.ctd to calculate the σ-profiles, σ-potentials, logarithmic activity coefficient at infinite dilution ($\ln\gamma$) and excess enthalpy. The software was a continuum solvation model to calculate the charge density on the surface of the molecule, and then solves the chemical potential in solutions, generating thermodynamic data. In the COSMO-RS calculations, an electroneutral approach to ILs was assumed, and ILs were treated as an equal ratio of cations and anions of 0.5 : 0.5. The calculation temperature was set to 25 °C, which was similar to the temperature used in the experimental validation for the dissolution of chitosan in ILs.

2.3 Structure of chitosan

The chemical structure of chitosan (2-dimensional) was drawn using MolView ver. 2.4 and is illustrated in Fig. 1, in which the –OH group present on C-2 and the $-NH_2$ group present on C-5 of the monomer of chitosan are the sites of formation of hydrogen bonds with the cations and anions of the ILs.

2.4 Structure of cations and anions

The chemical structures of the cations and anions employed in this study are included in Tables S1 and S2, respectively (ESI†). The cations were based on 20 amino acid cations and

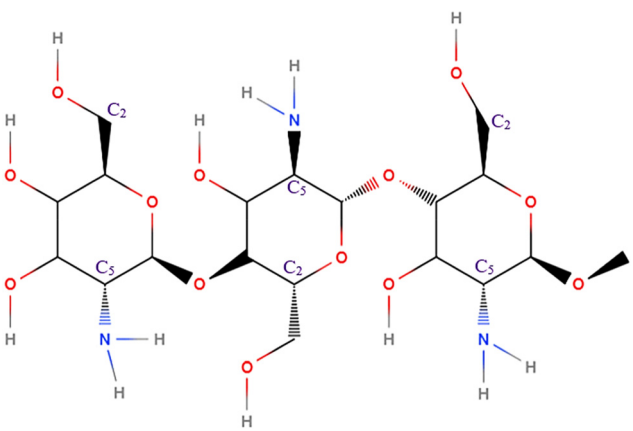

Fig. 1 Chemical structure of chitosan.

cations such as imidazolium, pyridinium, and pyrrolidinium with the alkyl chains of ethyl, butyl, hexyl, and octyl, respectively. The anions selected were carboxylates ($[C_2H_3O_2]$, $[C_4H_7O_2]$, $[CHO_2]$, $[C_6H_{11}O_2]$, $[C_8H_{15}O_2]$, $[C_3H_5O_2]$), aromatic carboxylates ($[C_7H_5O_2]$, $[C_7H_5O_3]$), halogens ([Br], [Cl], [I], $[BF_4]$), organic acids ($[C_3H_5O_3]$, $[C_2F_3O_2]$), sulphur-containing anions ($[C_4H_9SO_4]$, $[C_2H_6SO_4]$, $[HSO_4]$, $[C_8H_{17}SO_4]$, [SCN]), and nitrogen-containing anions ($[NO_3]$).

2.5 Experimental validation of COSMO-RS results

The top 5 ILs to dissolve chitosan were selected based on the lowest values of $\ln\gamma$ to validate the COSMO-RS results. These ILs were synthesized according to the methodology described by Tao *et al.*[39] with slight modification, in which an equimolar amino acid solution was refluxed with an equimolar inorganic acid at 60 °C for 24 h, and then recrystallized by dissolving the amino acid ILs in methanol/acetonitrile solution. Chitosan (Chemiz Malaysia, Selangor, Malaysia) with a minimum degree of deacetylation of 70% was used to validate the results obtained from COSMO-RS calculations, in which chitosan (1 wt%) was added to 5 g of ILs and stirred continuously at 250 rpm for 5 h in a silicon oil bath. Undissolved chitosan was removed by a dimethylsulfoxide (DMSO) treatment according to the procedures developed by Sun *et al.*[40] and expressed in terms of dissolution percentage (wt%).

3. Results and discussion

Conductor-like Screening Model for Real Solvents (COSMO-RS) is a robust and efficient tool to screen the appropriate solvents to dissolve polymers based on their thermodynamic properties. Parameters such as logarithmic activity coefficient at infinite dilution ($\ln\gamma$) and excess enthalpies (H^E) are associated with the dissolution ability and interactions between the solute and solvents, respectively.[36] Lower values of $\ln\gamma$ and H^E showed that the solute and the solvent can interact favourably with one another.

3.1 Sigma surface, profile and potential of chitosan

The screening charge distribution (σ surface) of chitosan is illustrated in Fig. 2(a), to assess the polarity and hydrogen bonding ability. In the charge distribution, red surfaces represent electronegative charges, green surfaces signify neutral charges, and blue surfaces are electropositive charges. Subsequently, the σ surface serves as an input in the calculations of COSMO-RS to determine the σ-profile and σ-potential of chitosan and predict the intermolecular and intramolecular interactions. σ-Profile refers to the degree of polarization of the structure of the molecule, representing the distribution of electron density around a molecule in a solvent, while σ-potential quantifies the affinity of a system to a polarity surface, which can be used to deduce the solvation free energy of a solute in a particular solvent.[41] Both the σ-profile and σ-potential is segmented into three sections: H-bond donor region ($\sigma < -0.082$ e A^{-2}), non-polar region (-0.082 e $A^{-2} < \sigma <$ 0.082 e A^{-2}) and H-bond acceptor region ($\sigma > 0.082$ e A^{-2}). Fig. 2(b) and (c) indicate the σ-profile and σ-potential of chitosan, respectively.

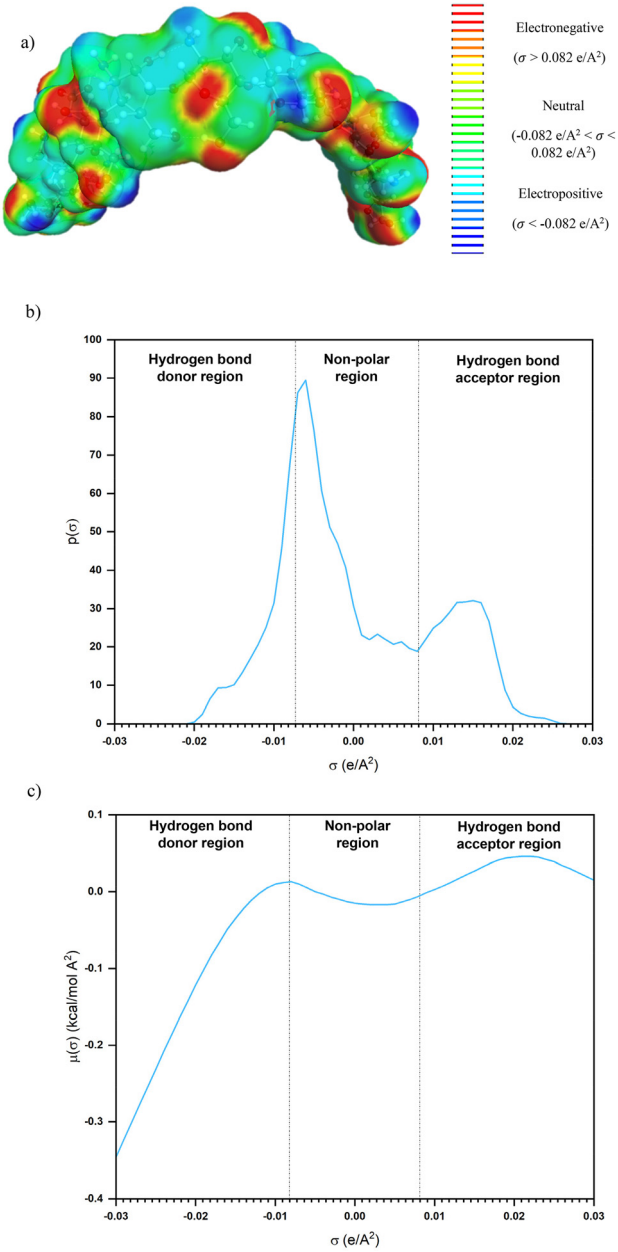

Fig. 2 σ-Surface (a), σ-profile (b), and σ-potential (c) of chitosan.

As shown in Fig. 2(a), chitosan has both positive and negative charges, which are attributed to the presence of amino groups ($-NH_2$) and hydroxyl groups (–OH), respectively. The distribution of the σ-profile in Fig. 2(b) demonstrated that chitosan possessed both H-bond donor and acceptor regions, as confirmed by the presence of blue surfaces (positively charged) and red surfaces (negatively charged) in Fig. 2(a), respectively. In the H-bond donor region, higher distribution of the screening charge density [$p(\sigma) = 80$] at -0.008 e A^{-2} indicated greater ability of –OH groups of chitosan to act as hydro-

gen bond donors. The screening charge distribution in the H-bond acceptor region was slightly lower and peaked at 40, which represents the ability of $-NH_2$ in chitosan to act as a hydrogen bond acceptor. This is true as there is only one functional NH_2 group in C-2 of a chitosan monomer, while there are two reactive –OH groups in C-3 and C-6 of a chitosan monomer.[42] The σ-potential of chitosan is illustrated in Fig. 2(c), with an increasing trendline in the interaction with H-bond donors and a decreasing trendline in the interactions with H-bond acceptors. Since chitosan has a weaker H-bonding accepting ability, it has decreasing interaction in the H-bond donor region, and its greater H-bonding donating ability is proved by an increasing interaction in the H-bond acceptor region.

The oxygen and hydrogen atoms present on the C-2 amino groups and C-5 hydroxyl groups of chitosan form electron donor–electron acceptor complexes with the cations and anions of ILs, disrupting the intermolecular and intramolecular hydrogen bonds within the chitosan polysaccharide chain, resulting in the detachment of amino and hydroxyl groups and subsequently dissolving the chitosan in the particular ILs.[26,43]

3.2 Screening of ILs for the dissolution of chitosan

By alternating each cation with the selected anions, a total of 640 ILs were constructed and assessed using the COSMO-RS based on their $\ln\gamma$ and H^E values, which are often quantitative traits to describe the dissolving capability of a solvent towards a particular solute. Lower values of $\ln\gamma$ and H^E indicated a more favorable interaction between chitosan and the ions of the ILs, bringing about better solvation power.[44]

Activity coefficient at infinite dilution ($\ln\gamma$) depicts the non-ideal behaviour of a solute purely due to the solute–solvent interaction,[45] in which lower values of $\ln\gamma$ mean that the solute and solvent are behaving more ideally following Raoult's law for ideal solutions. The values of $\ln\gamma$ of chitosan in all the 640 ILs are presented in Fig. 3(a), (b), (c), and (d), respectively.

From Fig. 3(a) and (b), it can be seen that the ILs with amino acid cations have the lowest $\ln\gamma$ values when coupled with $[BF_4]$ anions, except for the cations [Arg] and [His]. Amino acid ILs with [SCN] and $[C_2F_3O_2]$ have the second and third lowest activity coefficients, while amino acid ILs with [Cl] anions have the highest activity coefficient. Thus, $[BF_4]$ is selected as the anion of choice to synthesize amino acid ILs with varied cations. In Fig. 3(c) and (d), the general trend of cations based on imidazolium, pyridinium, and pyrrolidinium has the lowest $\ln\gamma$ values when coupled with these anions in descending order: $[C_2H_3O_2] > [C_3H_5O_2] > [C_4H_7O_2] > [C_6H_{11}O_2]$ with the increase in methylene chain length, and this effect is more prominent in pyrrolidinium ILs, followed by pyridinium, and lastly, imidazolium ILs. An increase in the values of $\ln\gamma$ in the screening of ILs for the dissolution of hemicellulose is also reported by Zhao *et al.*[34] with the elongation of the alkyl chain in both imidazolium and pyrrolidinium cations from the ethyl to octyl group, which supported our finding that the $\ln\gamma$ values of pyrrolidinium ILs were more influenced by the increase in alkyl chain length, as compared to imidazolium ILs. The highest $\ln\gamma$ values were observed when these cations were coupled with $[BF_4]$ anions, which has the opposite trend as observed in amino acid cations. This is due to the high hydrophobicity of these ILs, such as $[EMIM][BF_4]$.[46] Chitosan is hydrophilic in nature, due to the abundance of –OH and $-NH_2$ groups in its polymer chain, making them highly polar. Zheng *et al.*[46] observed that the interaction energy between H_2O-$[EMIM][BF_4]$ is positive, indicating that the formation of new H-bonds between the water and ILs is energetically weak and ineffective in dissolving polar solutes such as chitosan because the hydrophobic interactions are incapable of breaking the stronger polar bonds in chitosan.

The contribution of cations can be perceived in the values of $\ln\gamma$ values in the cations based on amino acids, and not as significant in the imidazolium, pyridinium, and pyrrolidinium cations. When comparing ILs with similar anions, for example, the $[BF_4]$ anion, the cation [Ser] has the lowest $\ln\gamma$ values, demonstrating the highest capability of $[Ser][BF_4]$ to dissolve chitosan. This is followed by the cations [Gly], [Cys], [Phe], and lastly, [Asn], ranked from the second to the fifth ILs with the greatest potential to dissolve chitosan.

According to Guo *et al.*[47] and Liu *et al.*,[33] the dissolution of polymers was mainly influenced by the type of anions, while cations had much less of an influence based on the difference in the values of $\ln\gamma$. However, in this study, the values of $\ln\gamma$ at infinite dilution of chitosan in amino acid-based ILs suggested that both cations and anions play equal roles in controlling the solubilization of chitosan in ILs. This has a good agreement with Mohan *et al.*[36] on the dissolution of PET plastic in ILs. According to Mohan *et al.*,[36] either one of the ions is expected to be a good hydrogen bond acceptor or donor, while the other ion could be slightly polar to weakly coordinate the counterion. Therefore, the interaction between chitosan and the ions of ILs is more substantial than the interactions between the cations and anions, leading to more chitosan being dissolved in the respective ILs. The same phenomenon has been observed in the dissolution of cellulose in guanidium-based ILs by Kahlen *et al.*,[32] when the guanidium cation is coupled with a weakly solvating anion such as $[PF_6]$. This combination is predicted to be one of the ILs that can best dissolve cellulose. Our results showed a similar trend, in which highly polar cations such as [Ser], [Gly], [Cys], [Phe], and [Asn], when coupled with usually weakly coordinating anions such as $[BF_4]$, are known to be the best ILs to dissolve chitosan due to the incoordination of the cations and anions of ILs and more favourable interactions between the chitosan and the individual ions present in the ILs. Hence, in this study, these five amino acid cations ([Ser], [Gly], [Cys], [Phe], and [Asn]) will be thoroughly investigated throughout the rest of the discussion.

3.3 σ-Profile of cations and anions

The σ-profile of cations and anions was computed to deduce the underlying interactions between chitosan and the ions constituting the ILs. The σ-profile of the top 5 amino acid

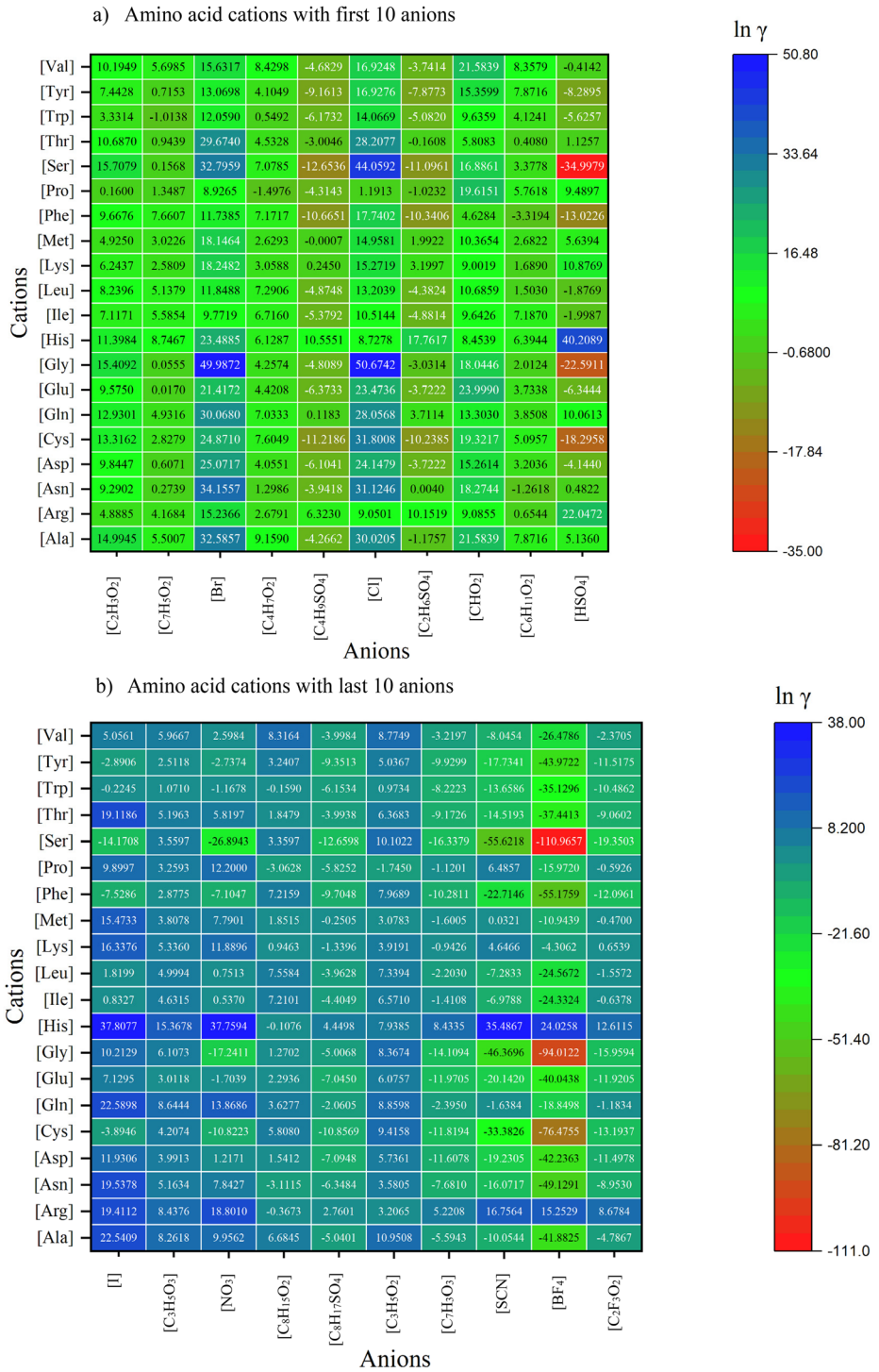

Fig. 3 Logarithmic activity coefficient at an infinite dilution (ln γ) of 640 ILs.

cations and chitosan is illustrated in Fig. 4(a) and (b), respectively, while the individual σ-profile of all the screened cations is shown in Fig. S1(a), S1(b), S1(c), S1(d), and S1(e),† respectively. Based on Fig. 4(a) and (b), the top 5 amino acid cations can interact with chitosan in all three regions: H-bond donor, and non-polar and H-bond acceptor regions, indicating that cations do play an important role in affecting the chitosan dissolution. These cations can interact favourably with chitosan and the respective anion due to the sharp peaks and huge area within the H-bond donor region. However, the cations only interact with chitosan in the non-polar region, indicated by a large area of the σ-profile of chitosan within the region, as opposed to the near-to-absence peak of the [BF_4] anion. The cations with a lower ln γ such as [Ser] and [Gly] have a smaller

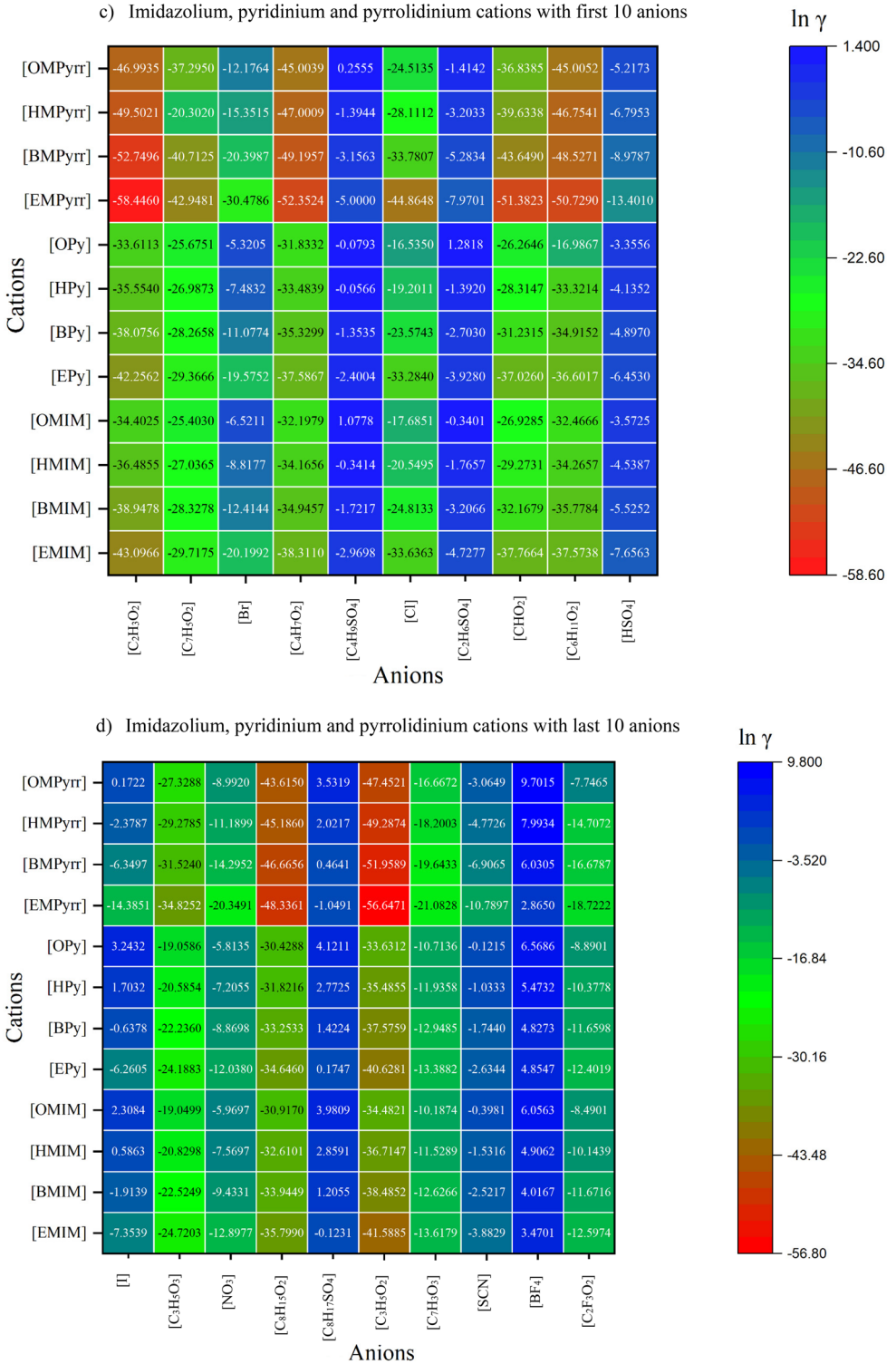

Fig. 3 *(Contd)*.

area in the non-polar region, as compared to the other amino acid anions such as [Phe], [Asn], and [Cys]. Thus, the main interaction of [Ser] and [Gly] cations with the chitosan and the anions is through polar interaction. All five amino acid cations can also interact with chitosan and the anion within the H-bond acceptor region with a single peak around 0.008 to 0.019 e A^{-2}. Overall, the σ-profiles of all the cations have a high overlapping region with chitosan due to the high polarity and various functional groups of amino acids, indicating greater dissolving ability of the amino acid ILs.

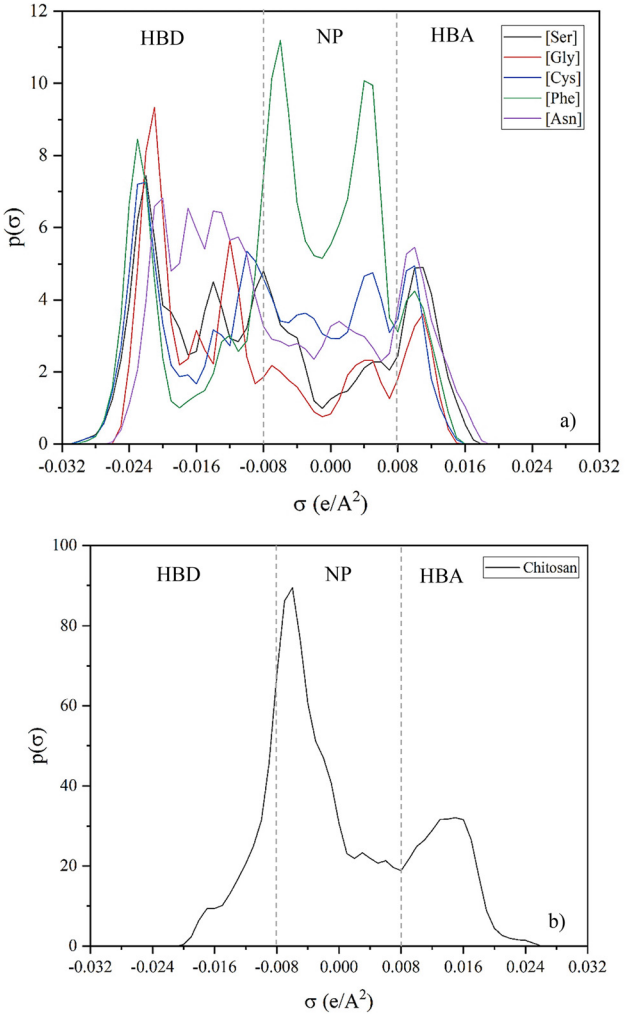

Fig. 4 σ-Profile of the top 5 amino acid cations (a) and chitosan (b).

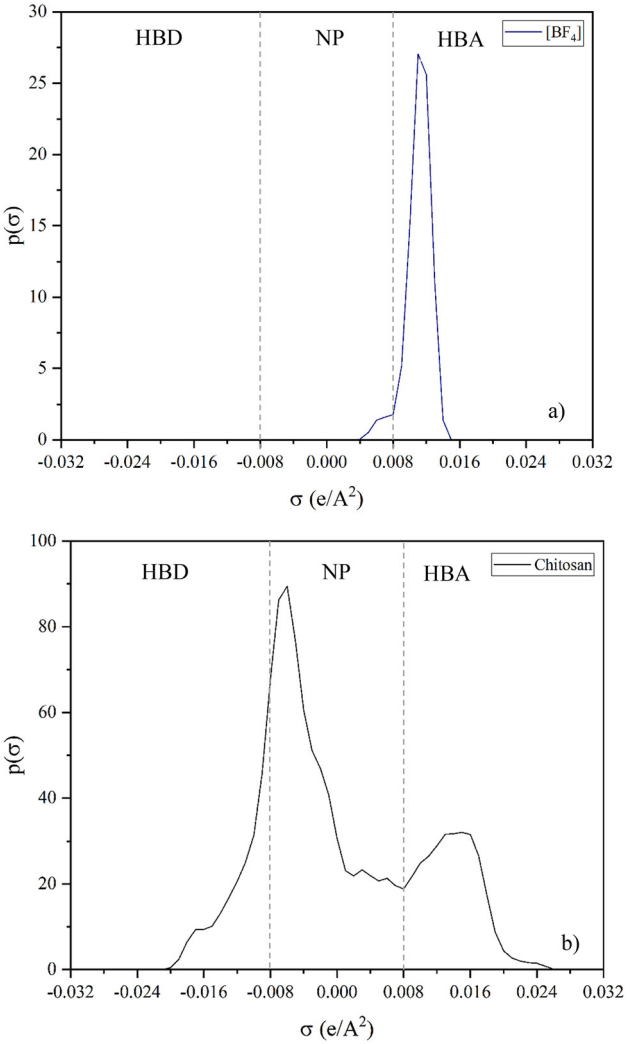

Fig. 5 σ-Profile of the [BF_4] anion (a) and chitosan (b).

The σ-profile of cations such as imidazolium, pyridinium, and pyrrolidinium [Fig. S1(d and e)†] only showed interactions in the H-bond donor and non-polar region, proving the superiority of the interactions between amino acid cations and chitosan. The effects of cations in the dissolution of chitosan are compared in Fig. S1(d) and S1(e),† using the cations [EMIM], [EPy], and [EMPyrr], depicting a similar range of peaks in the σ-profile with a slightly different peak intensity, indicating that the cations have a moderate effect on the dissolution of chitosan, which was also reported by Liu *et al.*[33] in assessing the σ-profile of [EMIM], [EPy], and [EEMor] cations in the dissolution of keratin.

The σ-profile of the [BF_4] anion and chitosan is shown in Fig. 5(a) and (b), respectively, while the σ-profile of all the 20 anions is depicted in Fig. S2(a), S2(b), and S2(c),† respectively. Tetrafluoroborate, [BF_4], anion has a very small peak around 0.004 to 0.008 e A^{-2} and a very sharp peak with a high intensity in the H-bond acceptor region from 0.008 to 0.016 e A^{-2}, which shows a favourable interaction between [BF_4] with chitosan and amino acid cations. All the anions have great complementarity with chitosan in the H-bond acceptor region [Fig. S2 (a–c)†], referring to their ability to act as H-bond acceptors and interact with H-bond donors such as the amino (NH_2) groups in chitosan and the amino acid cations.

3.4 Excess enthalpy (H^E) of ILs

Excess enthalpy (H^E) is associated with the individual contributions of intermolecular interactions such as hydrogen bonding, misfit interaction and van der Waals forces between chitosan and the ions of the ILs. Hydrogen bonding refers to the interaction where a hydrogen atom is covalently attached to a highly electronegative atom and interacts with the lone pair electrons of another electronegative atom, leading to a molecular cluster formation. Hydrogen bonding interaction is greater than the van der Waals force when dealing with polar compounds and is especially important in dissolution studies. Misfit interactions are especially significant in a mixture of molecules with different shapes and sizes, such as the interaction between the cations and anions and the chitosan mole-

cule, which is caused by the non-ideal changes during the dissolution reaction and arises when $\sigma + \sigma'$ is not zero.[30] van der Waals forces are the product of fluctuations in electron distribution around molecules due to London dispersion forces and dipole–dipole interactions gained during the transfer from the gas to the liquid phase.[48]

The values of H^E of the selected 5 ILs ([Ser][BF_4], [Gly][BF_4], [Cys][BF_4], [Phe][BF_4], and [Asn][BF_4]) were derived from the COSMO-RS model and are visualized in Fig. 6, while the values of H^E of all the 640 ILs are tabulated in Table S4.† It should be noted that dissolution of chitosan in ILs is desirable with a negative H^E value, indicating an exothermic reaction, whereby heat is released to the environment.

From Fig. 6, it is apparent that H^E is driven mainly by hydrogen bonding interaction in all the 5 ILs, ranging from 37% to 50% contribution. This was followed by the van der Waals forces being the second major contributor in [Gly][BF_4], [Phe][BF_4] and [Asn][BF_4], while misfit interactions were the second contributing factor to H^E in [Ser][BF_4] and [Cys][BF_4]. Similar findings were also reported Liu *et al.*[44] on the dissolution of cellulose and Mohan *et al.*[36] on the dissolution of polyethylene terephthalate (PET) plastics, in which both the authors agreed that the dissolution potential of a solute in ILs is dominated by hydrogen bonding, while misfit and van der Waals forces being the secondary factors in determining the enthalpy change.

In ILs with the same anions such as [BF_4], alteration in the cations constituting the ILs only resulted in slight differences in the values of H^E, which was in accordance with previously published data by Liu *et al.*,[33] stating that ILs with the same cations but different anions such as [Emim][$C_2H_3O_2$] and [Emim][DEP] displayed huge differences in H^E, while there is no much difference among ILs with the different cations, such as between [Amim][Cl] and [Apy][Cl] and [HOEtmim][Br] and [HOEtpy][Br]. The results conclude that the anion variation is the key factor in determining the value of H^E, which in turn dictates the intermolecular interactions between the solute (chitosan) and the solvent (ILs).

The possible hydrogen bond interactions between the cation $[Ser]^+$ and anion $[BF_4]^-$ of ILs and chitosan are illustrated in Fig. S3 and S4,† respectively. The IL [Ser][BF_4] was selected as an example to represent the other 4 ILs for the interaction with chitosan molecules, due to the highest dissolution percentage of chitosan obtained through COSMO-RS screening and experimentally when dissolved in the respective IL. The $\delta+$ on the H atom in the $[Ser]^+$ cation can interact with other electronegative functional groups in chitosan, such as the –OH and $–NH_2$ groups, through hydrogen bonding. The $\delta-$ charge present on the F atoms of the $[BF_4]^-$ anion is able to form hydrogen bonds with the $\delta+$ charge present on the H atoms linked to both the –OH group and $–NH_2$ group of chitosan, respectively.

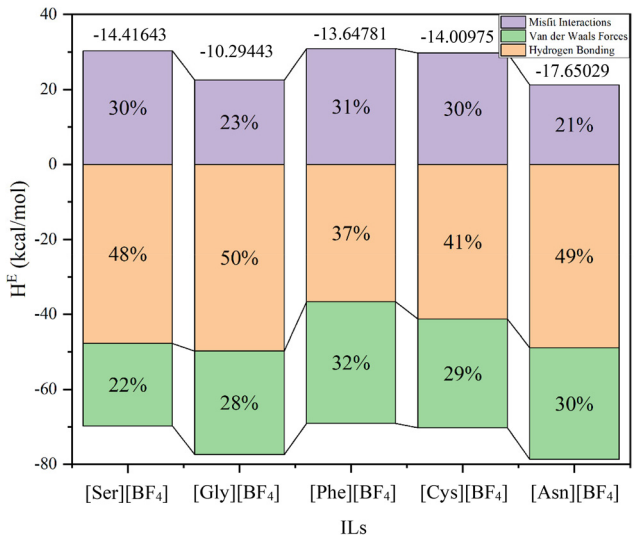

Fig. 6 Excess enthalpy (H^E) of the top 5 ILs.

3.5 Experimental validation of chitosan dissolution in the synthesized ILs

Typically, chitosan solution has been prepared using dilute acidic solutions such as acetic acid and its dissolution in more conventional ILs such as imidazolium-based ILs has been explored by various researchers in the past.[14,50] Acetic acid can be used to dissolve chitosan; however, the polymer undergoes degradation, causing changes to its physicochemical properties. This phenomenon was observed by Santoso *et al.*[49] in the experiment of dissolving chitosan in various concentrations of acetic acid at 40 °C for 30 minutes, where the group observed a reduction in the molecular weight of chitosan from 592.89 kDa to 198.64 kDa with the increase in acetic acid concentration from 1 to 5%, respectively. Our group has optimized the dissolution of chitosan in the same IL, [BMIM][Cl], and found that the optimized parameters were to dissolve 1 wt% of chitosan in 2 g of the ILs at a temperature of 130 °C for 72 hours.[50] However, conventional ILs were not favourable due to the requirement of high temperature and longer dissolution time, contributing to a greater production cost.

In this study, the dissolution of chitosan in the five synthesized ILs was conducted to validate the results obtained from the thermodynamic calculations of COSMO-RS. Approximately 1 wt% of chitosan was solubilized in 5 g of synthesized ILs with continuous stirring in a silicon oil bath at 250 rpm for 5 h. The results are tabulated in Table 1. It is cleared that the solubility of chitosan decreases as the values

Table 1 Preliminary screening of chitosan dissolution in ILs

Ionic liquids	Logarithmic activity coefficient at infinite dilution ($\ln\gamma$)	Dissolution percentage of chitosan (wt%)
[Ser][BF_4]	−110.9657	98.6
[Gly][BF_4]	−94.0122	90
[Cys][BF_4]	−76.4755	0
[Phe][BF_4]	−55.1759	89.2
[Asn][BF_4]	−49.1291	83

of $\ln\gamma$ increase, which is consistent with the predictive results obtained through COSMO-RS calculations, except for [Cys][BF_4]. This is because the IL [Cys][BF_4] is not stable and precipitated out during the process of regeneration of dissolved chitosan (as shown in Fig. 7). This has a good agreement with Liu *et al.*,[33,44] that the prediction of $\ln\gamma$ revealed that the preliminary screening of solute dissolution in ILs using COSMO-RS is reliable and in agreement with the experimental data.

The dissolution of chitosan in [Ser][BF_4] is also performed at two different temperatures, 25 and 50 °C, to study the effect of temperature in the dissolution process, and is tabulated in Table 2. At a fixed initial chitosan loading (1 wt%) and dissolution time (2 h), the dissolution percentage of chitosan increased from 98.20 to 100 wt% when the temperature increased from 25 to 50 °C. A similar increasing trend is also observed in the increase in dissolution percentage from 87.33 to 96.40 wt% by an increase in temperature from 25 to 50 °C, at a dissolution time of 8 h. This is because the increase in temperature decreases the viscosity of ILs, accelerating the swelling of chitosan, while promoting the mixing between chitosan and ILs, as also reported by Tan and Lee[51] in the dissolution of chitosan in [BMIM][Cl]. Besides that, a rise in temperature also resulted in the partial disruption of H-bonds.

Fig. 7 The white precipitate observed in chitosan-[Cys][BF_4] as compared to the translucent solution in chitosan-[Ser][BF_4].

Table 2 Dissolution of chitosan in [Ser][BF_4] at different temperatures

Run	Initial chitosan loading (wt%)	Temperature (°C)	Dissolution time (h)	Dissolution percentage (wt%)
1	1	25	2	98.20
2	1	50	2	100.00
3	1	25	8	87.33
4	1	50	8	96.40

4. Conclusion

In summary, an *a priori* screening method such as COSMO-RS was used to evaluate the dissolution capability of chitosan in 640 ILs. The values of $\ln\gamma$ suggested that both cations and anions played a major role in affecting the solubilization of chitosan. ILs with [BF_4] anions have the lowest $\ln\gamma$ and were ranked in the following order: [Ser][BF_4], [Gly][BF_4], [Cys][BF_4], [Phe][BF_4], and lastly, [Asn][BF_4]. These ILs were synthesized and validated experimentally. The dissolution of chitosan in all 5 amino-acid based ILs was exothermic, indicated by negative H^E values. The values of H^E for the ILs proposed that anions played a more significant role in influencing the intermolecular and intramolecular interactions between chitosan and the IL, which are dominated by hydrogen bonding, followed by misfit interactions and van der Waals forces. Experimental verification of chitosan dissolution in the 5 synthesized ILs was consistent with the predicted results obtained through the statistical thermodynamic calculations of COSMO-RS, which proved the reliability of COSMO-RS in screening the dissolution of chitosan in ILs, providing additional benefits in the processing of chitosan such as cost and time efficiency while reducing the wastage of chemicals concurrently.

Author contributions

Conceptualization: M. S.; data curation: S. Y. M.; formal analysis: S. Y. M.; funding acquisition: M. S.; supervision: M. S. and M. S. R. S.; validation: M. A. B. K. and Z. Z. A; writing – original draft: S. Y. M.; writing – review and editing: M. S. and M. S. R. S.

Conflicts of interest

There are no conflicts to declare.

Acknowledgements

This research was funded by the Ministry of Higher Education (MOHE) through the Fundamental Research Grant Scheme (FRGS/1/2021/STG01/QUEST/03/1). The authors would also like to extend their gratitude to QUEST International University and the Centre of Research in Ionic Liquids (CORIL), Universiti Teknologi PETRONAS for the laboratory facilities and computation tools provided.

References

1 D. Elieh-Ali-Komi and M. R. Hamblin, *Int. J. Adv. Res.*, 2016, **4**, 411–427.

2 V. Y. Novikov, S. R. Derkach, I. N. Konovalava, N. V. Dolgopyatova and Y. A. Kuchina, *Polymer*, 2023, **15**, 1729.
3 B. L. Bennett and L. Littlejohn, *Mil. Med.*, 2014, **179**, 497–514.
4 Z. Jiang, S. Wang, J. Hou, J. Chi, S. Wang, K. Shai, W. Liu, R. Sun and B. Han, *Carbohydr. Polym.*, 2020, **250**, 116994.
5 A. H. Najafabadi, M. Abdouss and S. Faghihi, *Mater. Sci. Eng., C*, 2014, **41**, 91–99.
6 Z. Nikfar and Z. Shariatinia, *J. Mol. Graphics Modell.*, 2017, **76**, 86–105.
7 G. Yuan, H. Lv, W. Tang, X. Zhang and H. Sun, *Food Control*, 2016, **69**, 818–823.
8 N. H. Mat Nayan, M. S. Anwar Hamzah, A. A. Mohd Tahir, A. A. Afina Rajali, E. F. Muslih and R. Mazlan, *J. Sci. Technol.*, 2018, **10**, 21–27.
9 I. Ito, T. Osaki, S. Ifuku, H. Saimoto, Y. Takamori, S. Kurozumi, T. Imagawa, K. Azuma, T. Tsuka, Y. Okamoto and S. Minami, *Carbohydr. Polym.*, 2014, **101**, 464–470.
10 H. Abd-Allah, R. T. A. Abdel-Aziz and M. Nasr, *Int. J. Biol. Macromol.*, 2020, **156**, 262–270.
11 P. Beulah, U. Jinu, M. Ghorbanpour and P. Venkatachalam, in *Advances in Phytonanotechnology From Synthesis to Application*, ed. M. Ghorbanpour and S. H. Wani, Academic Press, Cambridge, Massachusetts, 2019, pp. 329–341.
12 F. Shahidi and R. Abuzaytoun, *Adv. Food Nutr. Res.*, 2005, **49**, 93–135.
13 J. Kumirska, M. X. Weinhold, J. Thoming and J. Stepnowski, *Polymers*, 2011, **3**, 1875–1901.
14 H. Xie, S. Zhang and S. Li, *Green Chem.*, 2006, **8**, 630–633.
15 Z. Zhang, C. Li, Q. Wang and Z. K. Zhao, *Carbohydr. Polym.*, 2009, **78**, 685–689.
16 Q. Chen, A. Xu, Z. Li, J. Wang and S. Zhang, *Green Chem.*, 2011, **13**, 3446–3452.
17 X. Sun, Q. Tian, Z. Xue, Y. Zhang and T. Mu, *RSC Adv.*, 2014, **4**, 30282.
18 R. Feng, D. Zhao and Y. Guo, *J. Environ. Prot.*, 2010, **1**, 95–104.
19 Q. Zhao and J. L. Anderson, in *Comprehensive Sampling and Sample Preparation Analytical Techniques for Scientists*, ed. J. Pawlisyn, Elsevier, Amsterdam, Netherlands, 2012, pp. 213–242.
20 W. Wang, X. Ma, S. Grimes, H. Cai and M. Zhang, *Chem. Eng. J.*, 2017, **328**, 353–359.
21 S. Caporali, P. Marcantelli, C. Chiappe and C. S. Pomelli, *Surf. Coat. Technol.*, 2015, **264**, 23–31.
22 M. S. Raja Shahrom, C. D. Wilfred and A. K. Ziyada Taha, *J. Mol. Liq.*, 2016, **219**, 306–312.
23 A. Riisager, B. Jorgensen, P. Wasserscheid and R. Fehrmann, *Chem. Commun.*, 2005, **2006**, 994–996.
24 S. Li, S. Cai, W. Hu, H. Chen and H. Liu, *Spectrochim. Acta, Part B*, 2009, **64**, 666–671.
25 T. B. V. Dinis, F. Sousa and M. G. Freire, *Front. Bioeng. Biotechnol.*, 2020, **8**, 547857.
26 Z. Chen and Y. Wang, *Green Chem.*, 2011, **13**, 3446–3452.
27 S. N. Pedro, C. S. R. Freire, A. J. D. Silvestre and M. G. Freire, *Encyclopedia*, 2021, **1**, 324–339.
28 X. Zhang, Z. Liu and W. Wang, *Thermodynamics*, 2008, **54**, 2717–2728.
29 X. Zhao, Q. Yang, D. Xu, Z. Bao, Y. Zhang, B. Su, Q. Ren and H. Xing, *AIChE J.*, 2015, **61**, 2016–2027.
30 R. Anantharaj and T. Banerjee, *Ind. Eng. Chem. Res.*, 2010, **49**, 8705–8725.
31 A. S. Khan, T. H. Ibrahim, Z. Rashid, M. I. Khamis, P. Nancarrow and N. A. Jabbar, *J. Mol. Liq.*, 2021, **328**, 115387.
32 J. Kahlen, K. Masuch and K. Leonhand, *Green Chem.*, 2010, **12**, 2172–2181.
33 X. Liu, Y. Nie, Y. Liu, S. Zhang and A. L. Skov, *ACS Sustainable Chem. Eng.*, 2018, **6**, 17314–17322.
34 J. Zhao, G. Zhou, T. Fang, S. Ying and X. Liu, *RSC Adv.*, 2022, **12**, 16517.
35 Y. Cao, Z. Wu, Y. Zhang, Y. Liu and H. Wang, *J. Mol. Liq.*, 2021, **338**, 116778.
36 M. Mohan, J. D. Keasling, B. A. Simmons and S. Singh, *Green Chem.*, 2022, **24**, 4140.
37 L. Li, B. Yuan, S. Liu, S. Yu, C. Xie, F. Liu, X. Guo and S. Liang, *J. Appl. Polym. Sci.*, 2012, **123**, 3773–3780.
38 N. Taheri, A. Abdolmaleki and H. Fashandi, *Carbohydr. Polym.*, 2018, **195**, 413–419.
39 G. H. Tao, L. He, N. Sun and Y. Kou, *Chem. Commun.*, 2005, **2005**, 3562–3564.
40 N. Sun, M. Rahman, Y. Qin, M. L. Maxim, H. Rodriguez and R. D. Rogers, *Green Chem.*, 2009, **11**, 646–655.
41 A. Klamt, F. Eckert, M. Hornig, M. Beck and T. Burger, *J. Comput. Chem.*, 2002, **23**, 275–281.
42 J. Zhang, W. Xia, P. Liu, Q. Cheng, T. Tahirou, W. Gu and B. Li, *Mar. Drugs*, 2010, **8**, 1962–1987.
43 A. Pinkert, K. N. Marsh, S. Pang and M. P. Staiger, *Chem. Rev.*, 2009, **109**, 6712–6728.
44 Y. Liu, K. Thomsen, Y. Nie, S. Zhang and A. S. Meyer, *Green Chem.*, 2016, **18**, 6246–6254.
45 P. Alessi, M. Fermeglia and I. Kikic, *Fluid Phase Equilib.*, 1991, **70**, 239–250.
46 C. Zheng, Z. Shen, J. Zhou, Y. Pei and B. Yang, *Chem. Eng. Technol.*, 2021, **45**, 266–274.
47 Z. Guo, B. Lue, K. Thomasen, A. S. Meyer and X. Xu, *Green Chem.*, 2007, **9**, 1362–1373.
48 K. A. Kurnia and J. A. P. Coutinho, *Ind. Eng. Chem. Res.*, 2013, **52**, 13862–13874.
49 J. Santoso, K. C. Adiputra, L. C. Soerdirga and K. Tarman, *IOP Conf. Ser.: Earth Environ. Sci.*, 2020, **414**, 012021.
50 S. Y. Mok, M. Sivapragasam and M. S. Raja Shahrom, *Pertanika J. Sci. Technol.*, 2023, **6**, 3013–3038.
51 H. T. Tan and K. T. Lee, *Chem. Eng. J.*, 2012, **183**, 448–458.

